Peer-reviewed version available at *Polymers* **2020**, *12*, 1438; doi:10.3390/polym12071438

Optical Trajectory Manipulations Using the Self-Written Waveguides Technique

Ra'ed Malallah [1,2*], Derek Cassidy[1], Min Wan[1], Inbarasan Muniraj[1], John J. Healy[1] and John T. Sheridan[1*]

[1] School of Electrical and Electronic Engineering, College of Engineering and Architecture, University College Dublin, Dublin, Ireland.
[2] Physics Department, Faculty of Science, University of Basrah, Garmat Ali, Basrah, Iraq.

*Corresponding Authors: *e-mail: john.sheridan@ucd.ie
*Tel: +353-1-716-1927; Fax: +353-1-283-0921

Abstract: In this paper, first the Self-Written Waveguide (SWW) process in wet photopolymer media (liquid solutions), are examined for three examples: single-, counter-, and co-fibers exposure. Then the SWWs formed inside solid material are examined including the effects of manipulating the alignment of the fibers. In all cases high precision measurements are used to position the fiber optic cables (FOCs) before exposure using a microscope. The self-writing process is indirectly monitored by observing (imaging) the light emerging from the side of the material sample during SWW formation. In this way the optical waveguide trajectories formed in an Acrylamide/Polyvinyl Alcohol (AA/PVA) a photopolymer material (sensitized at 532 nm) are examined. First the transmission of light by this material is characterized. Then the bending and merging of the waveguides which occur are investigated. The predictions of our model are shown to qualitatively agree with the observed trajectories. The largest index changes taking place at any time during the exposure, i.e. during SWW formation, are shown to take place at the positions where the largest exposure light intensity is present. Typically, such maxima exist close to the input face and the first maximum is referred to as the location of the *Primary Eye*. Other local maxima also appear further along the SWW and are referred to as *Secondary Eyes*, i.e. deeper within the material.

Keywords: Self-Written Waveguide, Photo-polymer, Fiber Optics

Peer-reviewed version available at Polymers 2020, 12, 1438; doi:10.3390/polym12071438

1. Introduction

Many different types of self-process photopolymer materials have been studied for use in fabricating self-writing waveguides (SWWs) [1-3]. Such materials have several advantages: Large stable index changes can be obtained during exposure. They typically exhibit reproducible photosensitivity that occurs rapidly (seconds). These characteristics facilitate the investigation of self-writing by producing consistent experimental results and make them suitable for device applications [4-6]. Other advantages include optical quality (relatively low scatter), low cost, good spatial frequency response and in the case of volume gratings high diffraction efficiency [7, 8].

Kewitsch *et al.* [9] were the first to demonstrate that self-written structures can form in a photopolymer. It was however observed that the material response had non-ideal characteristics. Such material effects, e.g. dye absorption, constrain photopolymer material development and application [10-12]. To maximize the potential of these materials, deeper insights into the photo-physical and photo-chemical evolutions taking place during photo-polymerization (throughout the material volume with time), are necessary. Studies have been performed to examine the use of SWWs in photopolymers to couple, (including repairing by self-healing) between optical fibers, to form micro-tips at the end of optical fibers, to create biologically inspired microstructures and to implement strain sensors [2, 7, 13-15]. All of these applications require high-contrast refractive-index changes and high recording sensitivity, both of which can be provided by photopolymers [7]. It should also to be noted however that many recent studies into self-guided (self-trapped) optical beams have involved beams propagating in slab waveguides or nonlinear bulk media [16]. It has been observed that during exposure the exposing intensity distribution varies spatially and temporally inside the material. The innate tendency of optical beams is to diffract (spread) as they propagate in a homogeneous medium. However, this diffraction can be compensated for in a photopolymer material as the refractive index increases in the locally exposed regions during beam propagation [16]. SWW processes have previously been studied because of their possible use to produce steerable self-induced waveguides. For example, one beam is used to steer other beams in the same (attract) or different (repel) directions. In most cases it is desirable to record permanent SWWs. Ideally a highly photosensitive material which generates stable long-lasting refractive-index changes in response to illumination at a specific wavelength, are needed [17, 18]. In this paper, the optical properties required for a material host SWWs, are discussed.

The work presented here is organized as follows: First, wet photosensitive materials (liquid solutions) which have been previously examined for SWW formations are introduced. In this section the new studies for using the wet photosensitive materials are explained. The advantages of using dry materials are indicated. This section includes a discussion of the self-writing mechanisms and an investigation into the nonlinearity of our photosensitive material. The novelty for using thin drop cast layer of dry photosensitive materials (using microscopic distances) are studied intensively. The experimental set-up and material preparation procedures

Peer-reviewed version available at Polymers 2020, 12, 1438; doi:10.3390/polym12071438

used are presented. Then several waveguiding structures are fabricated. Finally the model used for the simulations is described, and a comparison of the measured and predicted results carried out.

2. Self-written waveguide evolution

The self-writing process is indirectly monitored by observing the transmitted light distribution emerging from the output of the sample during the exposure. It is also examined by capturing images of the light scattered from the sample side, (along the waveguide path). In our experiments the output beam is initially observed to narrow and become more intense during exposure as the index within the material increases with the formation of the SWW [18, 19].
A 3D model (combining material and electromagnetic effects), is necessary to describe SWW creation as the exposing light beam distribution in *x* and *y* propagates through a photopolymer material. As the light propagates in the *z* direction, the rate (partial differential) equation, that governs the spatial and temporal ground state photosensitizer concentration, can be given by [18, 19]:

$$\frac{\partial[A(x,y,z,t)]}{\partial t} = \frac{\partial}{\partial x}\left\{D_A(x,y,z,t)\frac{\partial[A(x,y,z,t)]}{\partial x}\right\} + \frac{\partial}{\partial y}\left\{D_A(x,y,z,t)\frac{\partial[A(x,y,z,t)]}{\partial y}\right\} + \frac{\partial}{\partial z}\left\{D_A(x,y,z,t)\frac{\partial[A(x,y,z,t)]}{\partial z}\right\} + k_r\left[Dye^*(x,y,z,t)\right] - k_a(x,y,z,t)[A(x,y,z,t)]. \quad (1)$$

$[A(x,y,z,t)]$ and $[Dye^*(x,y,z,t)]$ (mol cm^{-3}) denote the ground and excited states of the photosensitizer respectively. $D_A(x, y, z, t)$ (cm^3 mol^{-1} s^{-1}) is the diffusion rate of the ground state photosensitizer. The rate of production of the excited state photosensitizer is given by $k_a(x, y, z, t)$ (s^{-1}). The effects of dye diffusion $D_A(x, y, z, t)$ are assumed negligible, due to the relatively slow diffusion of the large dye molecules, compared to the other process taking place [20, 21]. It is also assumed that during the exposure the dye recovery is negligible, i.e., $k_r \approx 0$, being much faster than the recovery rate [22, 23].

Initially, the refractive index and absorptivity, inside photosensitive material, are considered to be homogeneous. Assuming linearly polarized monochromatic incident light, the electric field can be described by, $\boldsymbol{E}(x,y,z,t) = E(x,y,z,t)\,\hat{x}\,exp\{i(n_o k_o z - \omega t)\}$, where $E(x, y, z, t)$ is time varying amplitude of the electric field. n_o is the initial average refractive index of the homogenous medium, $\omega = 2\pi c/\lambda$ the light angular frequency and the wave number in free space is $k_o = 2\pi/\lambda$ [24-26], where λ is the free space wavelength. In this case, propagation in the material is governed by the paraxial wave equation [27, 28]:

$$\frac{\partial^2 E}{\partial z^2} + 2ik_0 n_0 \frac{\partial E}{\partial z} + \nabla_\perp{}^2 E + 2k_0{}^2 n_0 \Delta n E + 2k_0{}^2 \Delta n^2 E + ik_0 n_0 \alpha E = 0, \quad (2)$$

where $\nabla_{\perp}^{2} = \partial^2/\partial x^2 + \partial^2/\partial y^2$ denotes the 2-D Laplace operator, and $\Delta n(x, y, z, t)$ is the refractive index change. The index in the material is $n = n_0 + \Delta n$. The absorption parameter is defined by $\alpha = \mu c\sigma/n_0$, where μ and σ are the permeability and conductivity of the medium respectively, and c is the speed of light [2, 15, 29, 30]. A simple approximate phenomenological model has been typically used to describe the refractive index change induced during the self-writing process [2, 29, 30]:

$$\frac{\partial \Delta n(x, y, z, t)}{\partial t} = A_s I^p(x, y, z, t)\left(1 - \frac{\Delta n(x, y, z, t)}{\Delta n_s}\right), \tag{3}$$

The constant Δn_s denotes the maximum (i.e. saturation) value of the refractive index change in the particular medium being studied. The local light intensity is described by $I(x, y, z, t) = |E(x, y, z, t)|^2$. The number of photons that are involved in the process of photo-polymerization is typically assumed to be $p = 1$ [29]. A_s is a real coefficient that depends on the material used, i.e. the value of p, and the wavelength of the exposing light [2, 29, 30]. Eq. (3) is used to model the material photopolymerization process because it can be relatively easily combined with the paraxial wave equation Eq. (2) to provide satisfactory predictions. Therefore, it is reasonable to use this simple equation to approximate describe the temporal and spatial index changes during photopolymerization [2, 9]. However in free radical photo-polymerization systems, a more accurate model should involve calculating the individual material component concentrations using the related kinetic equations. $\Delta n(x, y, z, t)$ can then be calculated using the Lorentz-Lorenz formula. The phenomenological model, Eq. (2), is used because it is simple and the resulting predictions have been shown to agree reasonably well with the experimental results [18, 31-33].

In this work, the phenomenological model developed can be used to predict both the evolution of the light intensity distribution and the channel formation inside the material during the exposure [19, 32, 33]. The results obtained using the improved model provide a more detailed description of the waveguide evolution. Several characteristics observed within the material during the self-writing process are then predicted by the modified model. Behaviors of both wet and dry samples, during the SWW process, are examined. This work is performed in relatively thin drop cast layers over small propagation distances (microscopic distances), and an exposing power of P_0= 0.1 mW (i.e. each fiber has P_0 = 0.1 mW). The simplest case of self-writing exposing beam profile is examined. All cases studied involve the use of a Gaussian mode as the writing beam, i.e. the writing beams are input using single mode optical fibers. The material preparation for the cases examined here is described in detail in [34].

The experimental system used is illustrated in figure 1, with an actual setup inset. A green laser beam (532 nm) is divided into two beams using a beam splitter (BS). Then, each beam is coupled, into single-mode (SM) Fiber Optic Cable (FOC) type (P1-460B-FC-5) using Microscopic Objective lenses (MO) (Olympus/RMS4X) and Fiber Adapters (FA) (Qioptiq/G067054000). In the experiments, the two fibers are attached to a microscopic slide glass with theirs ends aligned (using Luminos, Optical Fiber Alignment Stage) and pointing

Preprints (www.preprints.org) | NOT PEER-REVIEWED | Posted: 5 September 2019 doi:10.20944/preprints201909.0064.v1

Peer-reviewed version available at Polymers 2020, 12, 1438; doi:10.3390/polym12071438

toward each other, (each fiber produces a Gaussian beam with P_0 = 0.1 mW). The photopolymer material is drop cast between the ends of the optical fibers so that it fills the space between them, see figure 1. The process of SWW formation was monitored using a microscopc (BRESSER Biolux NV 20x-1280x). Initially the desire was to observe whether the medium exhibited the ability to interconnect the fibers and therefore possibly other integrated optical devices. Silica based photopolymer materials have been used to combine integrated optical devices [35]. Typically the core size of the waveguide formed are in the region of ~9 µm, with an index difference between the core and cladding of ~10^{-3}. The Numerical Aperture (NA) of such a single mode fiber will typically be in the range, $0.05 \leq NA \leq 0.15$. The minimum bending radius of the waveguide fundamentally depends on the core size [36].

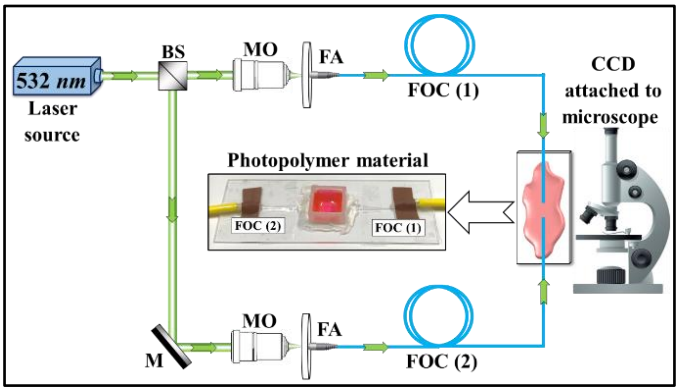

Figure 1. Optical setup for observing self-written waveguide formating through photopolymer material in order to observe dual single-mode fiber optic beams exposure.

The photopolymer material, as used in this work [13], consists of several components: A binder (Polyvinyl Alcohol-PVA), a monomer (Acrylamide-AA), a cross-linker (Bisacrylamide-BA) and an electron donor (Triethanolamine-TEA). The dye used here is Eosin-Yellowish (EY) ($C_{20}H_6Br_4Na_2O_5$), which is photo-sensitive to green light at wavelength λ = 532 nm, and acts to initiate the polymerization process [12, 21, 37]. A Gaussian beam at this wavelength emerges from the SM fiber inside the photosensitive material, see figure 1. The light propagates into the photosensitive material. The resulting refractive index changes generated due to polymerization make the SWW index higher than that of the surrounding material. Self-focusing will take place [38, 39]. Stable SWWs are formed if the exposing wavelength induces long lasting refractive index changes.

3. Results and discussion

In order to predict waveguide formation and therefore be able to optimize fabrication, the evolution of the refractive index distribution needs to be experimentally monitored. However, during the self-writing experiments, there is no simple method to directly measure the refractive index distribution induced in *x*, *y* and *z* with time without destroying the sample.

Preprints (www.preprints.org) | NOT PEER-REVIEWED | Posted: 5 September 2019 doi:10.20944/preprints201909.0064.v1

Peer-reviewed version available at Polymers 2020, 12, 1438; doi:10.3390/polym12071438

Therefore, we indirectly observe waveguide formation by measuring the transmitted and scattered light.

In this paper, the self-writing processing is examined for two phases (liquid and solid) of the same material. First, the behaviours of SWW inside liquid photopolymer material is studied for three cases, single-propagating beam, counter-propagating beams, and co-propagating beams exposures. Second, SWW formed inside solid material layers (as above) in which mis-alignment of the fibers is involved. In all cases the FOCs are positioned with microscopic accuracy. The self-writing process is indirectly monitored by observing the light emerging from the sides of the material sample during exposure. As the SWW forms, this imaged light narrows and become more intense as the index within the material increases in response to the waveguide formation. Numerical simulations of the self-writing process are performed and compared to the observed results.

3.1. Liquid photopolymer:

First, the liquid photopolymer material is examined. The preparation of the photopolymer material has been discussed in [34]. The material composition and reparation is similar to that used for holography. Single-mode optical fibers, having core diameters of 9μm, (125μm for the cladding), were used in the configurations examined. The optical fibers were placed on the microscope slide (25mm × 75 mm), using an optical fiber linear translation stage (Luminos, optical fiber alignment stage). The photopolymer material was then drop cast over the two optical fibers (or one optical fiber) as illustrated in figure 2. A small shallow chamber pool was formed around the gap between the fibers, (the walls of this pool are made by cutting 2-4 mm off the top of a cuvette), to make sure they were covered by sufficient photopolymer material. Green laser light (532 nm, 0.1 mW) was then used to expose the material. The optical fiber cables held in place attached by tape to the microscopic glass substrate (in the particular arrangement used for each study). Then, the photopolymer solution was drop cast to cover the fiber cable under dark room conditions. All experimental observations are captured using a microscope (BRESSER Biolux NV 20x-1280x).

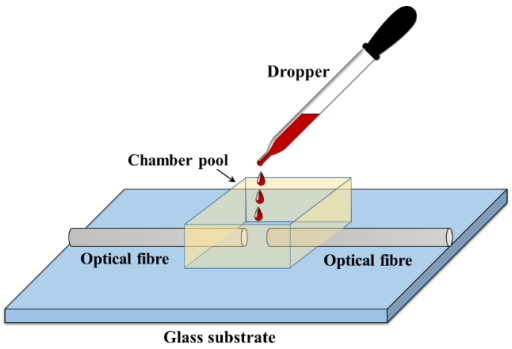

Figure 2. Drop cast photopolymer solution onto the gap between optical fibers ends.

Preprints (www.preprints.org) | NOT PEER-REVIEWED | Posted: 5 September 2019 doi:10.20944/preprints201909.0064.v1

Peer-reviewed version available at Polymers 2020, 12, 1438; doi:10.3390/polym12071438

In this case, exposure first acts to reduce the amount of inhibitor oxygen and eventually polymerization takes place. The free radical chains generated eventually terminate. Eventually dense polymer material, having a higher refractive index is formed. An irregular pattern is formed which is observed to be discolored and have a spherical shape, see figure 3.

In figure 3 different variation of the exposing setup are used to examine the results for different types of illumination. In all cases spherical shaped staining within the photopolymer solution is observed. The three set of results, for the three arrangements of optical fibers examined, show the evolution of similar spherical staining at the same three exposure time intervals: 180s, 360s and 720s. The measured transmission, through the solution, is not like that found during the formation of SWWs. Even though the refractive index changes, it does not appear to change in a way which produces guiding. Rather the light is scattered, and the material acts to diffuse it, effectively obstructing the propagation of the light. Use of liquid solutions does not appear to provide a practical way to produce SWWs.

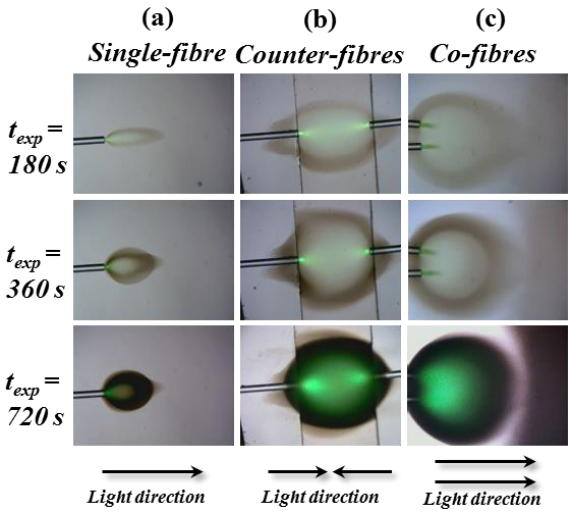

Figure 3. Microscope images of the spherical shapes created at the end of optical fiber (λ= 532 nm and P_0= 0.1 mW), inside the liquid photosensitive solution. There three exposing geometries involve illumination using: (a) Single-fiber; (b) Counter-fibers; and (c) Co-fibers. In each case the results for three exposing time: 180s, 360s and 720s are presented.

3.2. Solid photopolymer:

Solid photopolymer media are examined. In these cases the drop cast material, see figure 2, is allowed to dry to form a solid layer before exposure. Figure 4(a), shows the experimental result of an attempt to create a self-written optical waveguides using illumination from a single mode fiber optics (Gaussian intensity profile, P_0= 0.1 mW). Essentially the same set-up shown in figure 1 was used. The light beam is observed to expand (diverge) as it propagates in the solid homogenous medium. However eventually, as can be seen in figure 4(a) the light begins to focus to create a narrow channel that changes the beam intensity shape confirming the generation of a SWW. Therefore, the Gaussian beam is self-focused and self-trapped in the

Preprints (www.preprints.org) | NOT PEER-REVIEWED | Posted: 5 September 2019 doi:10.20944/preprints201909.0064.v1

Peer-reviewed version available at Polymers 2020, 12, 1438; doi:10.3390/polym12071438

optical waveguide channel along the direction of propagation inside the sample [3, 7, 21, 40, 41]. Thus, the diffraction of the light is balanced by the self-focusing effect and self-trapping occurs. These results can be compared to the corresponding numerical simulation shown in figure 4(b). The predictions in figure 4(b), show the light intensity distribution within the material at t_{exp}= 1600 s. The material is undergoing a physical change due to the propagating light being absorbed within the photosensitive material.

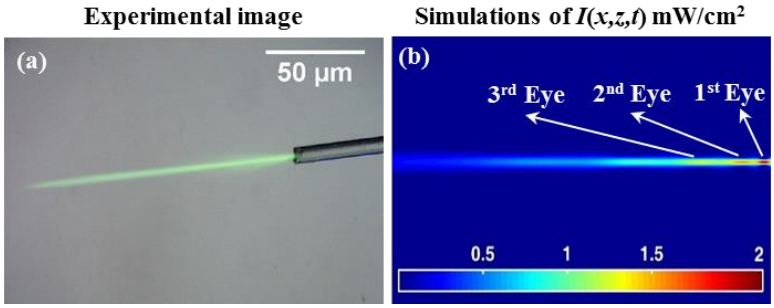

Figure 4. Light incident (from right to left) from a single mode optical fiber, t_{exp} = 1600 s of λ= 532 nm and P_0= 0.1 mW, (a) Experimental image results; and (b) Corresponding numerical intensity predictions, $I(x,z,t)$ mW/cm^2.

One effect identified during previous studies is the appearance of locations having high intensities during SWW formation. At some time t_0 early in the exposure a peak intensity is observed close to the face of the optical fiber, where light is input into the material. When $t_{exp} > t_0$ this peak moves along the propagation axis. This region of relatively higher intensity is referred to as the *Primary Eye* (1st Eye) and can be seen in figure 4(b) [42]. The presence of the *Primary Eye*, at a location within the material, indicates that the diffraction (spreading) of the propagating light is starting to be overcome by the increase in the refractive index along the waveguide path. We have observed that after initially forming, the *Primary Eye* moves forwards along the propagation axis, however later it is seen to move back towards the input face. As the exposure continues the index continue to evolve along propagation path [42].

As the refractive index increases and the SWW forms the cross-sectional refractive index (in the case of Gaussian beam illumination) increases all along the waveguide trajectory. Depending on the exposing intensity and the dye and monomer available the refractive index increases by different amount at different places. Due to these increases, new intensity maxima (local focus points) appear and these are referred to as *Secondary Eyes* (2nd and 3rd Eye). This growth in waveguide profile directly leads to the existence of the *Secondary Eyes* and their movement with time closer together and towards the input. The secondary eye appears to the right of the intensity primary eye (further away from the input). In the numerical simulations results, presented in figure 4(b), it can just be seen started to appear. It is also less localized (more spread out) along the SWW (in z) than the *Primary Eye*. To the left of the second eye (2nd) a third *eye* (3rd) eventually appears. The time and location at which the *Primary Eye* and *Secondary Eyes* form depends on the writing beam (intensity) as well as the material, e.g. the initial refractive index of the material and the maximum (saturation) index change that can be

Preprints (www.preprints.org) | NOT PEER-REVIEWED | Posted: 5 September 2019 doi:10.20944/preprints201909.0064.v1

Peer-reviewed version available at Polymers 2020, 12, 1438; doi:10.3390/polym12071438

induced within the material [42, 43]. As the refractive index profile continues to increase the waveguide will, during exposure, act more strongly on the light. This will lead to the appearance of more eyes, until eventually polymerization ends due to a lack of monomer. The model predicts a maximum percentage normalised transmission of light, for propagation of a distance of 80 μm, i.e. $(I_{out}/I_{in}) \times 100\%$ = 49.65%.

Next the formation of SWWs is examined when exposing using two parallel optical fibers, (co-fibers), separated by ~9.13 μm which simultaneously expose the AA/PVA with a power intensity P_0 = 0.1 mW (i.e. each fiber has P_0 = 0.1 mW) at λ= 532 nm, see figure 5(a). The corresponding predictions of the theoretical model are presented in, figure 5(b). We note that there is good qualitative agreement between the experimental results and the numerical predications. This suggests that our model reasonably well describes the dynamical photochemical and optical processes taking place within the material over the time period examined.

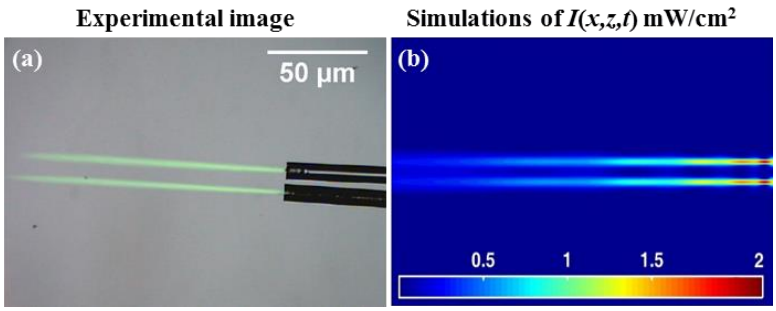

Figure 5. (a) Experimental observation (from right to left) for SWW form by exposure, t_{exp} = 1600 s of λ= 532 nm and P_0= 0.1 mW (i.e. each fiber has P_0 = 0.1 mW), two parallel single mode fiber optical cables, (b) Simulated light intensity distributions, $I(x,z,t)$ mW/cm^2.

The experimental image was generated along the two waveguide trajectories (path) within the sample. The image contains light scattered out from the material, but at least some light is absorbed during expose and then re-emitted. In the images captured some of the subtle features of the exposing light pattern occurring during the self-writing process, such as the appearance of the *Primary* and *Secondary Eyes*, which are predicted by the model, can be observed [42]. The two waveguides formed in this case follow separate parallel paths during the self-writing process, (shown when t_{exp} = 1600 s). They are parallel, exhibiting no convergence, divergence, or bending of their trajectories. The theoretical predicted value of maximum percentage normalized transmission for both beams is identical 49.65% for propagation distances of 80 μm (for each beam), the same as in the single beam case. Therefore, the two trajectories do not appear to interact and are independent of one another. Such an arrangement of writing fibers can be used for many potential applications [2, 7, 13-15].

To further investigate the processes of self-writing, the outputs of two single mode optical fibers were next carefully aligned and arranged facing each other, see figure 6. Once again the FOCs are placed onto a glass plate, held in place by tapes and a solution of photopolymer drop

Preprints (www.preprints.org) | NOT PEER-REVIEWED | Posted: 5 September 2019 doi:10.20944/preprints201909.0064.v1

Peer-reviewed version available at Polymers 2020, 12, 1438; doi:10.3390/polym12071438

cast on to them under dark room conditions. The photopolymer solution covering the fibers was then left to dry, for 24 hours.

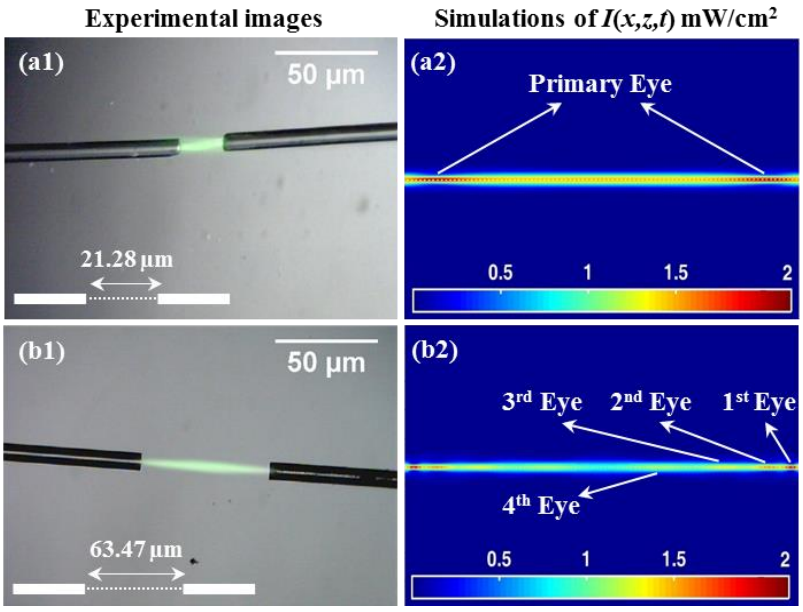

Figure 6. SWW for coupling using counter-propagation beams from single mode optical fibers. t_{exp} = 1600 s of λ= 532 nm and P_0= 0.1 mW (i.e. each fiber has P_0 = 0.1 mW). FOCs are aligned and separated by: (a) 21.28 µm, and (b) 63.47 µm.

The two optical fibers are positioned separated by gaps of 21.28 µm, in figure 6(a), and by 63.47 µm, in figure 6(b). All the measurement values listed here (i.e. distances and angles) are calculated from image data using the ImageJ software package [44]. Two beams then expose the AA/PVA simultaneously from the optical fibers. The beam counter-propagating (in opposite directions) directly towards the opposite fiber. The resulting passive connection should operate equally well for beams travelling in either direction (reciprocity). The exposure process was continued for 1600 s (each fiber has P_0 = 0.1 mW) allowing the SWW process to complete (to saturation). i.e. after this time no further evolution of the channel was observed. The corresponding simulation results are presented in figure 6(a2) and figure 6(b2). Good qualitative agreement with the experimental results is observed. This technique of connecting two optical fibers is potentially very advantageous as light from the actual fibers "automatically" generates the optical waveguide channel. In the simulation, the movement of the symmetrically located eyes (due to both the left and right illuminations) can be seen along the propagation axis.

As noted, experiments were performed with fibers placed, (a) 21.28 µm apart, and (b) 63.47 µm apart. This enabled us to examine the effects of the separation distance on the process by comparing the results, see figure 6(a2) and figure 6(b2). In both cases simultaneous coherent exposures clearly produced waveguides. We also note that our model produces qualitatively consistent predictions. The model predicts the increase in optical power along the waveguide

as the two exposing beams meet and then cross. This can be seen in figure 6(b2) where the optical power level is identified by the colour. Yellow indicates the highest intensity value which occurs in the middle of the gap. In figure 6(a2) an increase in optical power can also be seen as the two beams cross.

In figure 6(a2) the two symmetrically located *Primary Eyes*, are shown appearing in the region in front of both optical fibers. In figure 6(b2) the *Primary Eye* (1^{st}) and a series of higher order eyes (2^{nd}, 3^{rd} and 4^{th}) can be identified positioned symmetrically along the SWW [40]. This indicates that the two counter-propagating beams are present and are being confined. The *Secondary Eyes* can be seen in figure 6(a2), but due to the short distance between the two fibers the intensity is more uniform across the gap. However as the gap between the two fibers increases, see figure 6(b2) the *Secondary Eyes* can be more clearly distinguish from one another as they are more widely separated. Using the model, it is possible to predict the maximum percentage normalised transmission, (the value for propagation to the mid-point). If $I_{in(1)}$ is the input intensity from the right and $I_{in(2)}$ is the corresponding intensity from the left. Then dividing the predicted central intensity, I_{mid}, by the sum of the two input beams ($I_{in(1)} = I_{in(2)}$) gives the fraction of light from each propagating that distance, i.e. $\{I_{mid}/(I_{in(1)} + I_{in(2)})\} \times 100\%$= 41.42% at z=10.64 µm, see figure 6(a2), and 33.73% at z=31.73 µm, see figure 6(b2).

In figure 7 we examine cases in which the input optical fibers were not aligned. In this way the ability of the photopolymer material to act so as to help direct the waveguide formation trajectories to produce a waveguide capable of connecting mis-oriented optical fiber cables is demonstrated. In figure 7(a) two optical fibers are examined separated by ~36.75 µm with a lateral displacement (or shafting) of ~5.34 µm. In the second case the optical fiber cables are separated by a distance ~36.32 µm, figure 7(b), however in this case they were not displaced but angled with respect to one another, having an angular difference of ~7.76°. Once again two identical light beams are simultaneously transmitted along the optical fibers and then propagate inside the drop cast photopolymer material layer. The fibers are oriented so that the beams do not exactly cross propagate. However theoretically they are predicted to produce a self-written waveguide, see figure 6. Clearly the two beams do interacted with each other during the process of SWW formation. The result is single waveguide rather than two separate waveguides. In effect the two waveguides converge, i.e. the trajectories bend toward one another. Therefore, a method to connect two separated and misaligned optical fibers has been demonstrated.

Preprints (www.preprints.org) | NOT PEER-REVIEWED | Posted: 5 September 2019 doi:10.20944/preprints201909.0064.v1

Peer-reviewed version available at Polymers 2020, 12, 1438; doi:10.3390/polym12071438

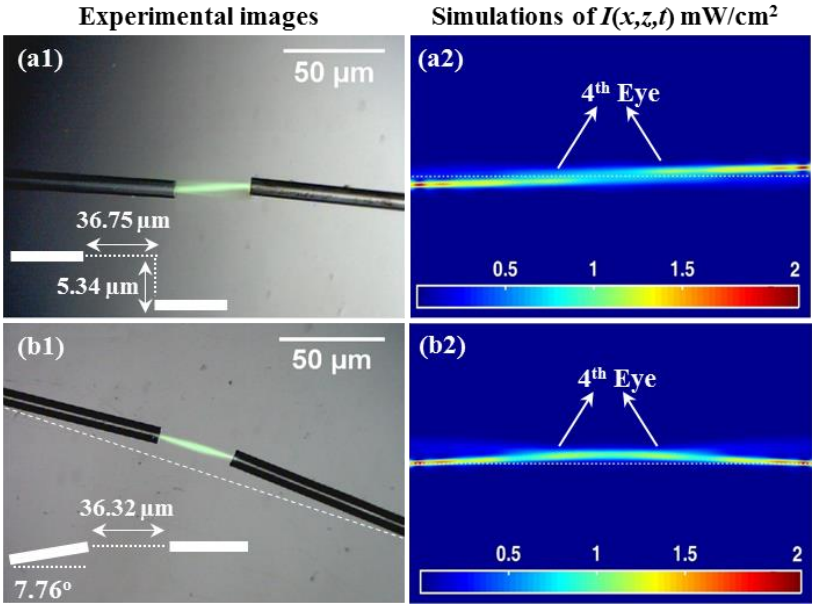

Figure 7. SWW for coupling single mode optical fibers, at t_{exp} = 1600 s of λ= 532 nm and P_0= 0.1 mW (i.e. each fiber has P_0 = 0.1 mW). Experiments and simulations: (a) Separated by 36.75 μm with shafting 5.34 μm, and (b) separated by 36.32 μm with angle 7.76°.

The experimental results are represented, in figures 7(a1) and (b1), and the corresponding predictions of our model, are shown in figures 7(a2) and (b2). There is good qualitative agreement. The model predicts the emergence of the *Primary Eye* and the *Secondary Eyes*. The symmetric appearance of eyes in both cases indicates that the two beams are involved in creating the connecting waveguides. The slight bending of SWW trajectories, which can be seen in both figures 7(a) and (b), indicates the path followed by the light within the waveguides formed. Clearly a connection is formed between the two optical fiber cables. Difficult opto-mechanical alignment which is currently needed for conventional fusion splicing or mechanical-splicing techniques, becomes less critical. Numerically it is predicted that the value of maximum percentage normalised transmission (in the mid distance between two beams), i.e. $\{I_{mid}/(I_{in(1)} + I_{in(2)})\} \times 100\%$, is calculated to be 22.63% at z=18.37 μm, see figure 7(a2), and 28.42% at z=18.16 μm, see figure 7(b2).

Figure 8 shows the situation in which two optical fibres are positioned side by side, separated by a distance of ~13.46 μm misalignment inwards at an angle of ~5.6°. The resulting waveguides formed within the photopolymer material is examined. Experiments and simulations are performed. The theoretical model also predicts, in agreement with the experiment results, that combination of the two waveguides into one will take place. Even though 4th and 5th Eye are lower values than the first eyes but they are visible and existent, see figure 8(b). The predicted existence of a 5th Eye indicates supports the claim that the two optical trajectories have combined as the total exposing optical power from both fibres is predicted to combine. To perform the experiment the two slightly misaligned fibres (relatively tilted by ~5.6°) were attached (by tape) to the microscopic slide. The photopolymer solution was then

Preprints (www.preprints.org) | NOT PEER-REVIEWED | Posted: 5 September 2019 doi:10.20944/preprints201909.0064.v1

Peer-reviewed version available at Polymers 2020, 12, 1438; doi:10.3390/polym12071438

drop cast. The two beam exposure then took place. In figure 8(b) the 5th Eye predicted to occur following the convergence of the two channels is highlighted. A *Y*-shaped junction is created which is analogous to *Y*-coupler cables used in optical networks. In this experiment the beams themselves generate the *Y*-combiner action.

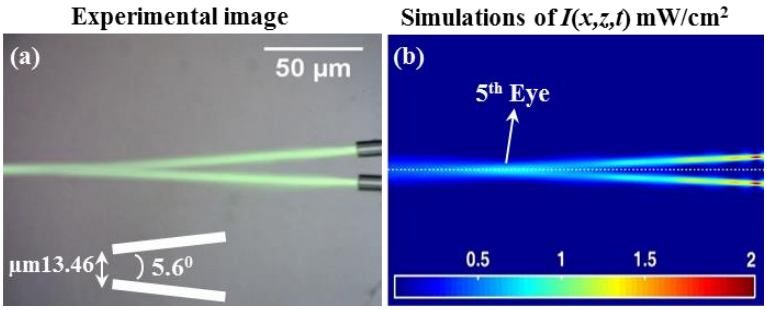

Figure 8. (a) Experimental observation image; and (b) Simulated light beam intensity, $I(x,z,t)$ mW/cm^2. Self-bending SWW behaviors for t_{exp} = 1600 s of λ= 532 nm and P_0= 0.1 mW (i.e. each fiber has P_0 = 0.1 mW). Two fibers initially separated by 13.46 μm and by an angle of 5.6^o. Formation of a *Y*-coupler (*Y*-waveguide). In all cases beams travel from right to left.

Based on our experimental results and also in our simulation software predictions, we have found that fibres separated by less than 9^o will always combine into a single channel. However, these beams will always cross each other when separated by more than 9^o, see figure 9(a). In figure 9 the predicted SWW structures, produced for another example, of two beam inputs, with different angular separation are presented. Increasing the angular separation to more than 9^o an *X*-coupling structure is formed, see figure 9(a). Figure 9(b) shows the structure predicted when the upper beam angle is greater than that of the lower beam but the angles between them is less than 9^o. This result is consistent with the result presented in figure 8 and a *Y*-coupler is formed. Such waveguide structures have many potential applications [2, 7, 13-15].

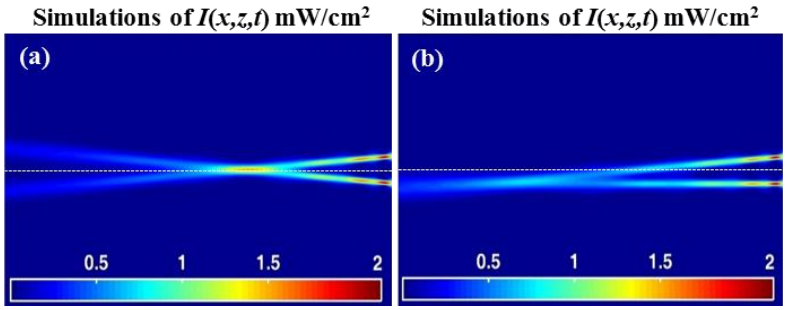

Figure 9. Predicted SWW structures, $I(x,z,t)$ mW/cm^2, formed at t_{exp} = 1600 s of λ= 532 nm and P_0= 0.1 mW (i.e. each fiber has P_0 = 0.1 mW) for (a) *X*-waveguide (>9^o) and (b) off-axis *Y*-waveguide (<9^o).

4. Conclusion

The possibilities created by the ability to fabricate self-written waveguides in photopolymer material has been further investigated. While recording in liquid solutions has been shown to be possible, the results are poor and permanent structures require the photopolymer material be solid. The photopolymer material used in this paper (sensitized at 532nm) is manufactured in our laboratory to strict guidelines. In this paper the formation of SWW in thin drop cast AA/PVA layers, is demonstrated. It is shown that the bending of the light trajectories during self-written waveguide formation can be used to form a wide range of potential useful photonic circuits. Experiments and simulations have been performed so as to understand self-bending phenomenon for different input beam (exposure) arrangements.

At first in this paper, the use of photopolymer solution (liquid) as a SWW media is examined. Three examples are studied: single-beam, counter-beams, and co-beams illumination. The results indicates that light scattering inside the solution does not produce stable SWWs. Next SWW formation, inside solid material layers, for mis-align fibers is examined. The self-writing process is indirectly monitored by observing the light emerging from the side of the material sample over time. Numerical simulations using the model developed were carried out. The result are all in good qualitative agreement with the experimental observations. The model is then available to simply explore situations more difficult to implement experimentally. Several interesting applications have been identified, including *Y*-junctions and *X*-junctions.

References:

[1] Sarkisov S. S., Grimalsky V., Curley M. J., Adamovsky G. and Martin C. 2001 *Proceedings SPIE* **4455**, 107-118.

[2] Bachelot R., Ecoffet C., Deloeil D., Royer P. and Lougnot D. J. 2001 *Applied Optics* **40**, 5860-5871.

[3] Jisha C. P., Kishore V. C., John B. M., Kuriakose V. C., Porsezian K. and Kartha C. S. 2008 *Applied Optics* **47**, 6502–6507.

[4] Yoshimura T., Roman J., Takahashi Y., Wang W. V. and Inao M., 2000 *Electronic Components & Technology Conference*, 962-969.

[5] Hirose N. and Ibaragi O., 2002 *Electronic Components and Technology Conference* **52**, 268–275.

[6] Sugihara O., Tsuchie H., Endo H., Okamoto N., Yamashita T., Kagami M. and Kaino T., 2004 *IEEE Photonics Technology Letters* **16**, 804-806.

[7] Dorkenoo K., Crégut O., Mager L., Gillot F., Carre C. and Fort A., 2002 *Optics Letters* **27**, 1782–1784.

[8] Suzuki N. and Tomita Y., 2004 *Applied Optics* **43**, 2125-2129.

[9] Moran J. M. and Kaminow I. P., 1973 *Applied Optics* **12**, 1964-1970.

[10] Kewitsch A. S. and Yariv A., 1996 *Optics Letters* **21**, 24–26.

[11] Odian G., 2004 *Principles of Polymerization*, 4th Edition Wiley, New York.

[12] Tolstik E., Kashin O., Matusevich A., Matusevich V., Kowarschik R., Matusevich Y. I. and Krul L. P., 2008 *Optics Express* 1**6**, 11253–11258.

[13] Jeong K. H., Kim J. and Lee L. P., 2006 *Science* **312**, 557-561.

[14] Huang H., Majumdar A. and Cho J.-S., *2009 Transactions of the Institute of Measurement and Control* **31**, 247-257.

[15] Qi Y., Gleeson M. R., Guo J., Gallego S. and Sheridan J. T., 2012 *Physics Research International* **2012**, 975948.

[16] Anderson A. and Peters K., 2009 *Journal of Lightwave Technology* **27**, 5529-5536.

[17] Sukhorukov A. A. and Kivshar Y., 2001 *Pramana-Bangalore* **57**, 1079-1096.

[18] Shoji S., Kawata S., Sukhorukov A. A. and Kivshar Y., 2002 *Optics Letters* **27**, 185–187.

[19] Li H., Qi Y., Malallah R. and Sheridan J. T., 2015 *Journal of the Optical Society of America* **B 32**, 912–922.

[20] Guo J., Liu S., Gleeson M. R. and Sheridan J. T., 2011 *Optical Engineering* **50**, 015801.

[21] Li H., Qi Y., Ryle J. P. and Sheridan J. T., 2014 *Applied Optics* **53**, 8086–8094.

[22] Gleeson M. R., Kelly J. V., Close C. E., O'Neill F. T. and Sheridan J. T., 2006 *Journal of the Optical Society of America* **B 23**, 2079–2088.

[23] Qi Y., Li H., Fouassier J. P., Lalevée J. and Sheridan J. T.,2014 *Applied Optics* **53**, 1052–1062.

[24] Siegman A. E., 1986 *Lasers*, University Science, Mill Valley, Calif.

[25] Gleeson M. R., S. Liu, O'Duill S. and Sheridan J. T., 2008 *Journal of Applied Physics* **104**, 064917.

[26] Kashin O., Tolstik E., Matusevich V. and Kowarschik R., 2009 *Journal of the Optical Society of America* **B 26**, 2152–2156.
[27] Tsao C., 1992 *Optical Fibre Waveguide Analysis*, Oxford University Press, Oxford.
[28] Kagami M., Yamashita T. and Ito H., 2001 *Applied Physics Letters* **79**, 1079–1081.
[29] Kewitsch A. S. and Yariv A., 1996 *Applied Physics Letters* **68**, 455–457.
[30] Monro T. M., Poladian L. and Sterke C. M., 1998 *Physical Review* **E 57**, 1104–1113.
[31] Kashin A. M. and Monro T. M., 2003 *Journal of the Optical Society of America* **B 20**, 1317–1325.
[32] Malallah R., Cassidy D., Muniraj I., Ryle J. P., Healy J. J., and Sheridan J. T., *Applied Optics* 57 (22), E80-E88, (2018).
[33] Malallah R., Li H., Muniraj I., Cassidy D., Al-attar N., Healy J. J., and Sheridan J. T., *Journal of the Optical Society of America* **B** 35(8), 2046-2056, (2018).
[34] Malallah R., Li H., Kelly D. P. and Sheridan J. T., 2017 *Polymers* **9**, 337.
[35] Ljungström A. M. and Monro T. M. 2002 *Journal of Lightwave Technology* **20**, 78-85.
[36] Murphy E. J., 1999 *Integrated Optical Circuits and Components: Design and Applications*, Marcel Dekker Inc., New York.
[37] Tolstik E., Romanov O., Matusevich V., Tolstik A. and Kowarschik R., 2014 *Optics Express* **22**, 3228–3233.
[38] Barthelemy A., Maneuf S. and Froehly C., 1985 *Optics Communications* **55**, 201-206.
[39] Qi Y., Li H., Guo J., Gleeson M. R. and Sheridan J. T., 2014 *Optics Communications* **320**, 114–124.
[40] Mitchell M., Chen Z., Shih M. and Segev M., 1996 *Physical Review Letters* **77**, 490–493.
[41] Guo J., Sheridan J. T. and Saravanamuttu K., 2013 *Journal of Optics* **14**, 035201.
[42] Svalgaard M., Poulsen C. V., Bjarklev A. and Poulsen O., 1994 *Electronics Letters* **30**, 1401-1403.
[43] Schneider C. A., Rasband W. S. and Eliceiri K. W., 2012 *Nature Methods* **9**, 671-675.
[44] Monro T. M., de Sterke C. M. and Poladian L., 1996 *Journal of the Optical Society of America* **B 13**, 2824-2833.